

Label-free DNA sensors using ultrasensitive diamond field-effect transistors in solutionKwang-Soup Song,^{1,2,3,*} Gou-Jun Zhang,³ Yusuke Nakamura,^{1,2} Kei Furukawa,^{1,2} Takahiro Hiraki,^{1,2} Jung-Hoon Yang,^{1,2} Takashi Funatsu,⁴ Iwao Ohdomari,^{1,2,3} and Hiroshi Kawarada^{1,2,3}¹*Department of Electronical Engineering and Bioscience, School of Science and Engineering, Waseda University, 3-4-1 Okubo, Shinjuku-ku, Tokyo 169-8555, Japan*²*Nanotechnology Research Center & Institute of Biomedical Engineering, Waseda University, Waseda Tsurumaki-cho 513, Shinjuku-ku, Tokyo 162-0041, Japan*³*Consolidated Research Institute for Advanced Science and Medical Care, Waseda University, Waseda Tsurumaki-cho 513, Shinjuku-ku, Tokyo 162-0041, Japan*⁴*Laboratory of Bio-Analytical Chemistry, Graduate School of Pharmaceutical Sciences, The University of Tokyo, 7-3-1 Hongo, Bunkyo-ku, Tokyo 113-0033, Japan*

(Received 24 May 2006; revised manuscript received 15 August 2006; published 27 October 2006)

Charge detection biosensors have recently become the focal point of biosensor research, especially field-effect-transistors (FETs) that combine compactness, low cost, high input, and low output impedances, to realize simple and stable *in vivo* diagnostic systems. However, critical evaluation of the possibility and limitations of charge detection of label-free DNA hybridization using silicon-based ion-sensitive FETs (ISFETs) has been introduced recently. The channel surface of these devices must be covered by relatively thick insulating layers (SiO₂, Si₃N₄, Al₂O₃, or Ta₂O₅) to protect against the invasion of ions from solution. These thick insulating layers are not suitable for charge detection of DNA and miniaturization, as the small capacitance of thick insulating layers restricts translation of the negative DNA charge from the electrolyte to the channel surface. To overcome these difficulties, thin-gate-insulator FET sensors should be developed. Here, we report diamond solution-gate FETs (SGFETs), where the DNA-immobilized channels are exposed directly to the electrolyte solution without gate insulator. These SGFETs operate stably within the large potential window of diamond (>3.0 V). Thus, the channel surface does not need to be covered by thick insulating layers, and DNA is immobilized directly through amine sites, which is a factor of 30 more sensitive than existing Si-ISFET DNA sensors. Diamond SGFETs can rapidly detect complementary, 3-mer mismatched (10 pM) and has a potential for the detection of single-base mismatched oligonucleotide DNA, without biological degradation by cyclically repeated hybridization and denature.

DOI: [10.1103/PhysRevE.74.041919](https://doi.org/10.1103/PhysRevE.74.041919)

PACS number(s): 73.40.Mr, 82.47.Rs, 82.80.Fk

I. INTRODUCTION

The detection of specific DNA relies on sensing of hybridization between functionalized probe DNA and its complementary target DNA [1–7]. Although many methods are available to detect the hybridization of DNA, fluorescent labeling-based microarrays are normally used [6]. However, eliminating the labeling steps is required to produce “gene chips,” providing a simple, accurate, stable, and inexpensive platform for patient diagnosis [7,8]. On the other hand, surface plasmon resonance (SPR) [9], quartz crystal microbalance (QCM) [10], and the mechanical cantilever array [11], which are label-free detection methods, achieve the highest sensitivity and decrease the analytical process (without labeling), but these methods require highly precise and expensive instrumentation.

In silicon-based, ion-sensitive field effect transistors (Si-ISFETs) the gate is a SiO₂/Si interface, where interfering cations (K⁺, Na⁺, and Ca²⁺) can easily cause deterioration of the electrical properties of the ISFETs. Therefore, encapsulation is a major concern in the design of Si-ISFETs to prevent the penetration of ions from the electrolyte into the channel.

The structure of the diamond solution-gate FETs (SGFETs) shown in Fig. 1(a) is based on a hydrogen-terminated surface having a *p*-type accumulation layer and is suitable for biosensors due to the passivation-free and membrane-free channel surface [12], which allows direct contact between biomolecules and the channel surface, subsequently resulting in ultrahigh sensitivity and high-speed detection. DNA immobilization has been reported on diamond thin films and powders [13,14]. Due to the strong surface chemical bonds, DNA immobilization and hybridization are free from biological interface degradation over time. Diamond surfaces meet the requirements of robust biosensing devices [15] as the surface shows chemical-physical stability [13,16] and a wide potential window [17], providing an insulating interface between electrolyte solution and solid for insulating gate field effect transistor (FET) operation.

II. MATERIALS AND EXPERIMENTS

Polycrystalline diamond films were synthesized on a *p*-type silicon substrate (100) by a microwave-plasma-assisted chemical vapor deposition (MPCVD) method using purified hydrogen [99.999%, 396 sccm (cubic centimeter per minute at standard temperature and pressure)] and methane (99.999%, 4 sccm) gas, purchased from Tokyo-Gas-Chemical Japan, at a pressure of 45 Torr, 1.2 kW, and

*Author to whom correspondence should be addressed. FAX: 81-3-5286-3391. Electronic address: song@kaw.comm.waseda.ac.jp

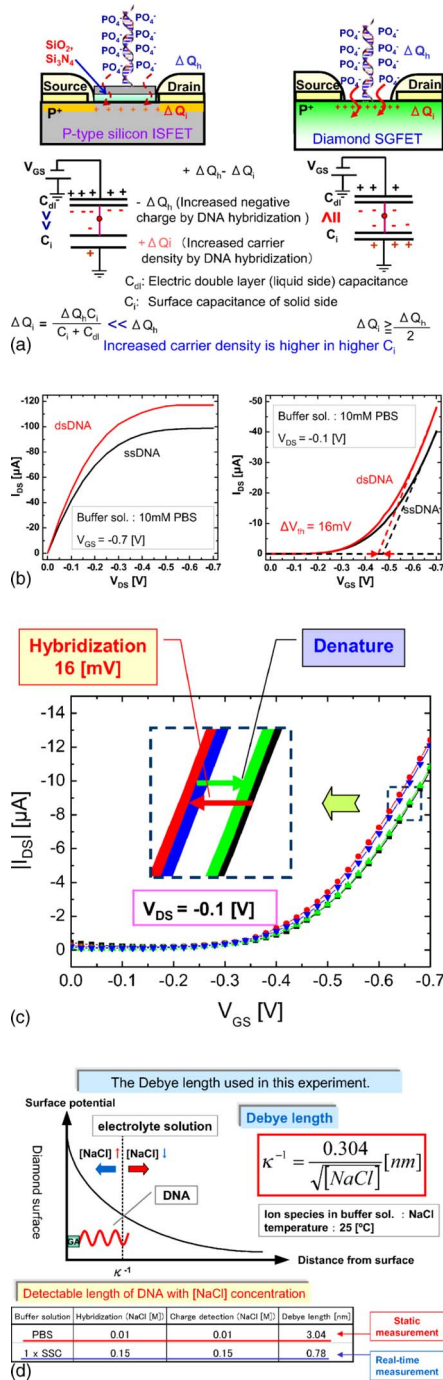


FIG. 1. (Color online) The static device characteristics of diamond SGFETs by hybridization and the mechanism of detecting signal depending on the Debye length. (a) Theoretically, diamond SGFETs show higher sensitivity to DNA charge than Si-ISFETs, because the channel surface is directly exposed to electrolyte solution without insulating layers. (b) The directly exposed channel surface is very sensitive to surface charge on diamond SGFETs. After hybridization with complementary target oligonucleotide on the functionalized channel surface, the surface negative charge increases and hole carrier density is enhanced due to the increased negative charge on the channel surface. (c) The sensitivity to detect DNA hybridization is stable about cyclic hybridization and denaturation on diamond SGFETs. (d) The Debye length compares to the concentration of NaCl in 1:1 electrolyte solutions.

840 °C for 12 h in a microwave plasma reactor (ASTEX 2115). The thickness of deposited diamond film was approximately 8 μm. After deposition, the diamond surface was hydrogenated by plasma treatment in an environment of hydrogen gas. The H-terminated diamond surface has a two-dimensional hole gas layer without doping (24), which is 10–20 kΩ/sq sheet resistance at room temperature and stable in the temperature range from 150 to 400 K in air. Diamond SGFETs were fabricated on the hydrogenated polycrystalline diamond film surface. Gold was evaporated through a metal mask on the H-terminated diamond surfaces to form drain and source ohmic contacts. Ar⁺ ions were implanted through a metal mask (Mo) to form an insulating region. Wires were bonded on the drain and source electrodes. Finally, drain and source electrodes were covered with epoxy resin to protect them from the electrolytes by hand [18]. The channel length and width were 500 μm and 8 mm, respectively.

Direct surface modification on the H-terminated diamond surface was performed with UV irradiation in an ammonia (99.999%) gas environment to generate amine sites on the channel surface. The wavelength of the UV light used (Halogen lamp) was 253.7 nm. Prior to UV irradiation, nitrogen gas has been introduced for 6 min to remove oxygen and other activated gases in the UV chamber. The amine sites have been produced directly on the H-terminated diamond channel surface. Spatially resolved XPS (monochromatic Al Kα X-ray 1486.7 eV source) was used for quantitative evaluation of the modified sites generated on the diamond surface by direct amination. All the chemicals and solvents were purchased from Kanto Chemical Co., Inc. (Tokyo, Japan) and used without any further purification. A reference electrode of Ag/AgCl was used as a gate electrode. The sequences of oligonucleotides (21-mer) purchased from the Sigma Genosys Japan are shown in Table I.

III. RESULT AND DISCUSSION

A. Static detection

The process of DNA immobilization and hybridization on the directly aminated diamond surface has been described in detail previously [19]. The distance between the oligonucleotide and the surface is crucial for detection of the negative charge of the phosphate groups on the sugar chains (phosphate backbone) in oligonucleotides, because the negative charge is neutralized by its conflicting positive ions in the electrolyte if the distance exceeds the Debye length [2,3,5]. In the direct amination method, this distance is shorter than in other methods [13,14,16]. Amine bonding is stable and its coverage is controllable by changing the corresponding UV irradiation time on the diamond surface.

Diamond SGFETs functionalized with a 21-mer probe oligonucleotide through 25% coverage of the directly aminated channel surface are characterized by drain current (I_{DS}-V_{DS}, V_{SG} = -0.7 V) and gate potential (I_{DS}-V_{DS}, V_{SG} = -0.1 V) in phosphate buffer saline (PBS) buffer solution (NaCl 10 mM, pH 7.4). The SGFET DNA biosensors are sensitive to hybridization at low ionic concentrations (10 mM) because charge detection is most sensitive when the screening of

TABLE I. Sequences of oligonucleotide DNA used in this experiment

	Sequence of 21-mer DNA oligonucleotides
Probe DNA oligonucleotide	H2N-5'-CCACGGACTACTTCAAAAATA-3'
Complementary target	3'-GGTGCCTGATGAAGTTTGTGAT-5'
Non-complementary target	3'-GCTAGCTAGCTAGCTAGCTAG-5'
3-mer mismatched target	3'-GGTGGCTGATTAAGTATTGAT-5'
1-mer mismatched target	3'-GGTGCCTGATTAAGTTTGTGAT-5'

positive counter ions (Na^+) is minimized in the electrolyte. Diamond SGFETs are hybridized with specific target oligonucleotide (10 pM) under the same conditions as used in a microarray [19]. After hybridization, drain current increased by 20 μA and gate potential showed a positive shift of 16 mV as compared to those with only the probe functionalized on the channel surface, as shown in Fig. 1(b). The probe oligonucleotide hybridizes with the complementary oligonucleotide and hole density is increased by the enhanced negative charge on the p -type channel surface. Consequently, the gate potential shows a positive shift and drain current increases. We repeat the hybridization (10 pM) and denature (in 8.3 M urea solution) cyclically. When the target oligonucleotide DNA is denatured in urea solution, the gate potential shifts negatively due to the decreased negative charge on the channel surface and positively shifts by rehybridization due to the increased negative charge, as shown in Fig. 1(c). The shift of gate potential is stable in the cyclic hybridization and denature.

The Debye length in aqueous solutions can be determined by the Graham equation, which is simplified for 1:1 electrolyte solutions [20], presented in Fig. 1(d). We used certain approximations to quantify the immobilized probe oligonucleotide on the channel surface. As the Debye length of buffer solution is 3 nm and the length of a 21-mer oligonucleotide is 6 nm, an 11-mer per individual oligonucleotide strand hybridized on the channel surface includes an intrinsic negative charge, which directly influences the channel surface without any neutralization by counter ions (Na^+) in the solution. The hybridization of DNA and its efficiency increase on a positively charged surface [21]. The H-terminated diamond surface is positively charged due to the surface dipoles ($\text{H}^{+0.06}\text{-C}^{-0.06}$). Six percent of the area density of surface hydrogen has a partial positive charge. Aminated diamond surface (NH_3^+) is also positively charged. This positively charged diamond surface accelerates hybridization and its efficiency increases to 10% ($1.1 \sigma_{DNA}$) at a target DNA concentration of 10 pM. According to the Debye-Huckel theory, the attachment of charge to surface should result in a corresponding surface potential change, which is described by the Graham equation [22]. The attachment of charged molecules to the channel surface will reduce the surface potential, and the resulting signal is transduced to the gate potential,

$$\Delta V_{GS} = \frac{2kT}{e} \left[\sinh^{-1} \left(\frac{\sigma_0 - \sigma_{DNA}}{\sqrt{8\epsilon_{elect}\epsilon_0 kTn_0}} \right) - \sinh^{-1} \left(\frac{\sigma_0 - 1.1\sigma_{DNA}}{\sqrt{8\epsilon_{elect}\epsilon_0 kTn_0}} \right) \right] \quad (1)$$

where k is the Boltzmann constant, T is absolute temperature, e is elementary charge, ϵ_0 is the permittivity of free space, ϵ_{elect} is the dielectric constant of water (78), n_0 is buffer ionic strength, σ_0 is surface charge density, and σ_{DNA} is surface-immobilized DNA charge density. As the coverage of amine is 25%, the corresponding density of amine is $2.5 \times 10^{14} \text{ cm}^{-2}$ [18]. The ratio of NH_2 and $-\text{N}=\text{C}-\text{H}$ after treatment with glutaraldehyde is 10% ($2.5 \times 10^{13} \text{ cm}^{-2}$). Consequently, σ_0 is $4.0 \times 10^{-6} \text{ C/cm}^2$ on the partially aminated diamond surface. Using the above equation, the change in gate potential (ΔV_{GS}) at 16 mV after hybridization corresponds to $0.29 \times 10^{-5} \text{ C/cm}^2$ (σ_{DNA}) and the immobilized probe oligonucleotide is estimated to be $3.3 \times 10^{12} \text{ cm}^{-2}$ when an 11-mer is effective in its intrinsic negative charge.

Figure 2(a) shows the sequential changes of drain current in hybridization, denature and 3-mer mismatch at incubation temperatures of 55 and 40 $^\circ\text{C}$. The drain current depends on the incubation temperature and the shift of drain current is higher at high temperature (55 $^\circ\text{C}$) on the complementary target DNA. In general, the hybridization probability is the highest 20–25 $^\circ\text{C}$ below the melting temperature ($T_m = 77 \text{ }^\circ\text{C}$) on the complementary target DNA-DNA hybridization [23]. Little drain current was observed reproducibly with noncomplementary target DNA, and a slight drain current was detected with a 3-mer mismatched DNA at lower incubation temperature. The probe DNA was hybridized with complementary and 1-mer mismatched oligonucleotide DNA (100 pM) at room temperature (25 $^\circ\text{C}$) and denatured in urea solution (8.3 M), cyclically, as shown in Fig. 2(b). At each cycle, gate potential is shifted positively by hybridization between complementary or 1-mer mismatched oligonucleotide DNA and probe DNA. The average shift in the complementary is 21 mV and that of 1-mer mismatch is 18 mV. The difference of the shifted gate potential between complementary and 1-mer mismatched oligonucleotide DNA is 3 mV. This is particularly important, because a potential application of DNA sensors is to detect DNA point mutations associated with disease. The gate potential returned to nearly the same level by denaturing but a little bit positive position. This shift might be caused by the negative surface charge accumulation such as by halogen ions [15] in the denaturing (initializing) process. In the present case the initialize gate voltages shifts positively and reaches to 5–6 mV. The precise denaturing process is necessary for the reliable hybridization sensing. However, this data is the first report on the sequential voltage shift by hybridization and denaturing in FET detection.

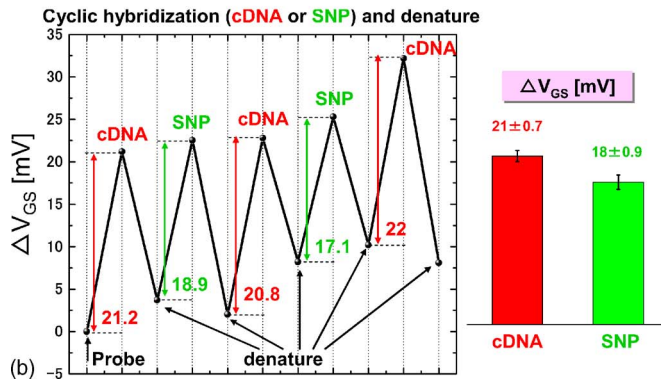
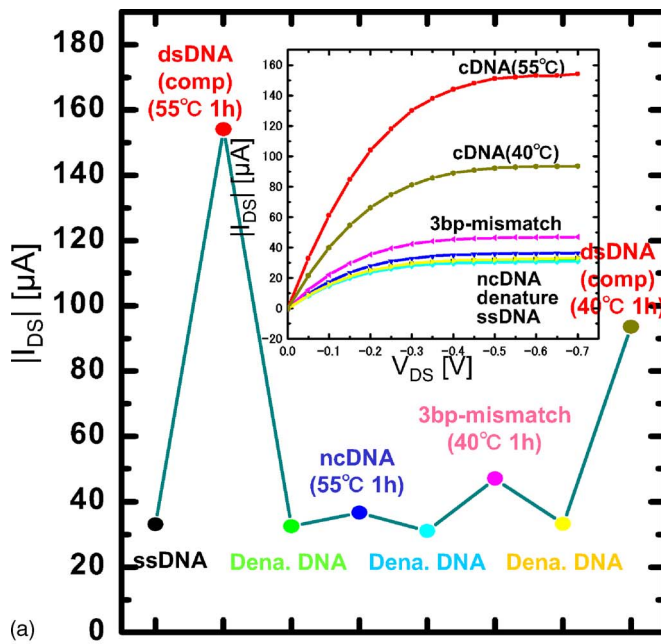


FIG. 2. (Color online) The sequential changes of gate potential and drain current in hybridization, and denature with complementary, 3-mer and 1-mer mismatched target DNA, respectively. (a) The sequential changes of drain current in hybridization and denature are stable and characteristic under various conditions. Drain current is characterized in 3-mer mismatched and complementary target oligonucleotide DNA by modifying the incubation temperature. (b) The shift of gate potential is different in complementary and 1-mer mismatched target oligonucleotide DNA at room temperature.

B. Real-time detection

Specific buffer solution ($1 \times \text{SSC}$: sodium saline citrate) is used for hybridization and detection of signals in real time at room temperature. Gate potential is measured in fixed drain current ($I_{DS} = -10 \mu\text{A}$) with $V_{DS} = -0.2 \text{ V}$ to detect hybridization. After stabilization in buffer solution, complementary 21-mer target oligonucleotide solution ($10 \mu\text{L}$, $1 \mu\text{M}$) was introduced with a micropipette, as shown in Fig. 3. Gate potential showed a positive shift by 38 mV after 100 s and the relevant response time was very fast, as shown in Fig. 4(a). We rinsed the channel surface with buffer solution ($1 \times \text{SSC}$). After rinsing, the gate potential did not shift back to the single-strand DNA (ssDNA) immobilized value. When

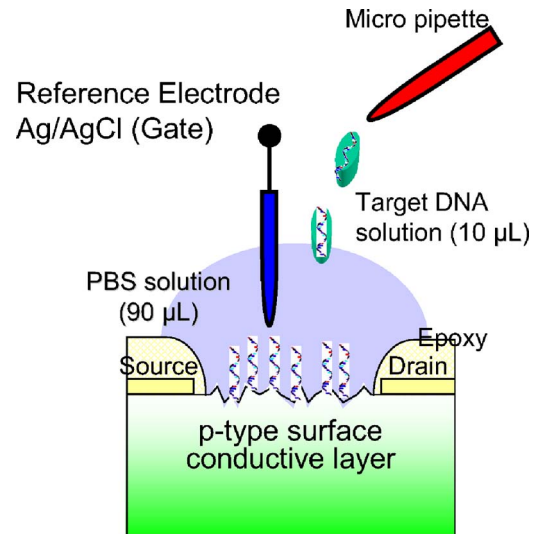


FIG. 3. (Color online) The introduction of target DNA solution on the channel surface of diamond SGFETs with real-time detection.

we changed the concentration of target oligonucleotide, the shift in gate potential decreased to 25 mV and 4 mV at target concentrations of 100 nM and 10 nM, respectively. The shift in gate potential increased depending on the annealing time at room temperature, as shown in Fig. 4(a). Hybridization increases in proportion to the concentration of DNA and annealing time [23,24]. In real-time detection, the sensitivity was low as compared to the static detection shown before, because we used a shorter Debye length buffer solution (0.78 nm) modified NaCl concentration inevitable for the rapid hybridization in the real-time detection. However, we demonstrated the possibility of *in vivo* diagnostics in real time using SGFETs.

Noncomplementary target oligonucleotide solution ($10 \mu\text{L}$, 100 nM) was introduced onto the channel surface. As shown in Fig. 4(b), the gate potential was shifted approximately 6 mV by nonspecific bindings. Nonspecific binding occurs on the channel surface in high concentrated target oligonucleotide solution, which results in a positive shift in the gate potential (6 mV). However, the shift of gate potential by nonspecific bindings is 6 mV in 100 nM concentrated noncomplementary target DNA solution, which is specifically distinguishable from that of 100 nM concentrated complementary target DNA solution (25 mV). We introduced the target DNA solution (100 nM, $10 \mu\text{L}$) to evaluate the physical adsorption on the H-terminated diamond surface without immobilization of probe DNA on the channel surface. After introduction of target DNA solution on the H-terminated diamond surface without probe DNA, the gate potential shifted to the positive direction by 3.4 mV, probably due to the physical adsorption on the H-terminated diamond surface, as shown in Fig. 4(b). At a concentration of 10 nM, gate potential shifted positively through nonspecific binding after 10 min for annealing, as shown in Fig. 4(c). The difference between specific and nonspecific binding increased to 7 mV after 20 min through the progression of hybridization. Figure 4(d) shows the changes of gate poten-

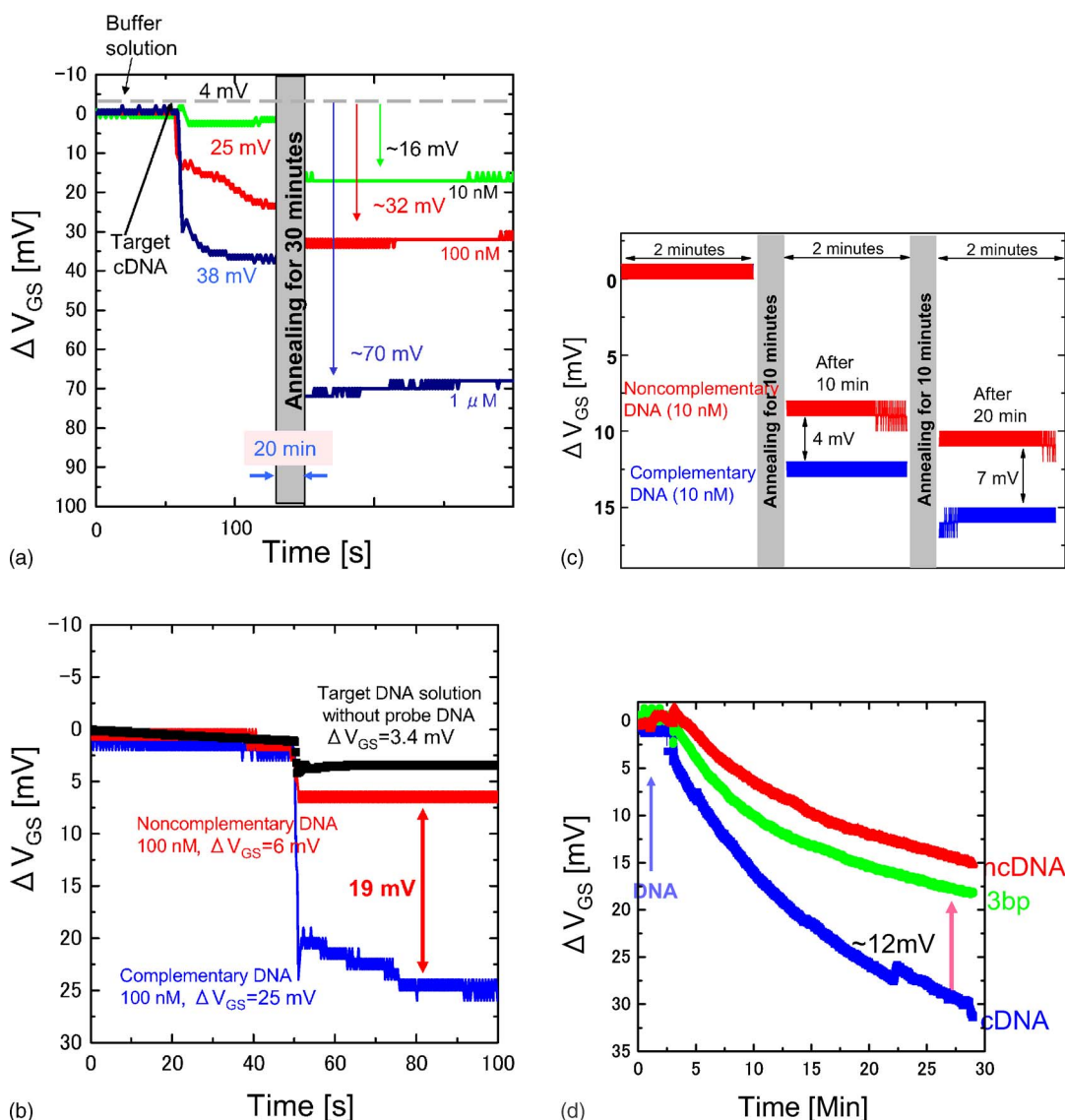


FIG. 4. (Color online) Real-time detection of complementary and noncomplementary target oligonucleotide DNA depending on the concentration and annealing time. (a) The shifted gate potential is enhanced by the concentration of complementary target oligonucleotide because the count density of hybridized oligonucleotide is increased. (b) Diamond SGFETs discriminate between complementary and noncomplementary oligonucleotide DNA in real-time detection, definitely. (c) The count of hybridized oligonucleotide DNA increases depending on the annealing time. The signal is a distinct difference between specific binding and non-specific binding in the target oligonucleotide DNA solution (10 nM). (d) The complementary target DNA hybridization is surely distinguishable compared 3-mer mismatched target DNA (100 nM).

tial in complementary, 3-mer mismatched, and noncomplementary target DNA hybridization at room temperature (25 °C), and the concentration of target DNA is 100 nM, in real-time detection. The signal of complementary DNA hybridization is surely distinguishable from those of noncomplementary and 3-mer mismatched DNA. The diamond SGFETs were immersed in urea solution (8.3 M) to denature the target oligonucleotide. When the target was denatured in urea solution, gate potential shifts negatively due to the decreased negative charge on the channel surface and returned to the original values. Denatured diamond SGFETs were rehybridized with complementary target oligonucleotide (10 μL, 100 nM). After rehybridization, the gate potential shifted positively by 24 mV, which was the same as in the

first hybridization. The stability of DNA immobilization and hybridization on the diamond surface due to strong chemical bonding was reported previously using label-conjugated DNA [13]. In the present study, potentiometric detection using SGFETs without labeling allows cyclic hybridization, denature, and rehybridization to be monitored with high sensitivity in real time. We have described a highly sensitive, directly electrical detection methodology to detect DNA hybridization of complementary, 3-mer mismatched, and noncomplementary DNA with cyclically repeated denature using diamond SGFETs in real time. In addition, concentration-dependent sensitivity of the shifted gate potential by DNA hybridization was characterized and shown to provide a rapid assay of relative stability, quick response, and high

sensitivity, which suggested that this approach could serve as a technology platform of diagnostics of disease and drugs in real-time detection.

C. Principal of DNA detection by diamond SGFETs

Diamond SGFETs are compared with Si ISFETs from the point of charge distribution in parallel capacitances. Figure 1(a) shows equivalent circuits of the two FETs with electric double-layer capacitance (C_{dl}) and channel surface capacitance of solid side (C_i). When target DNA is hybridized with probe DNA, the charge increase ($-\Delta Q_h$) appears between two capacitances and is reflected to the positive charge increase in the two sides according to the ratio between two capacitance C_i and C_{dl} in a solution. The increased carrier (charge) density by DNA hybridization is shown in the following.

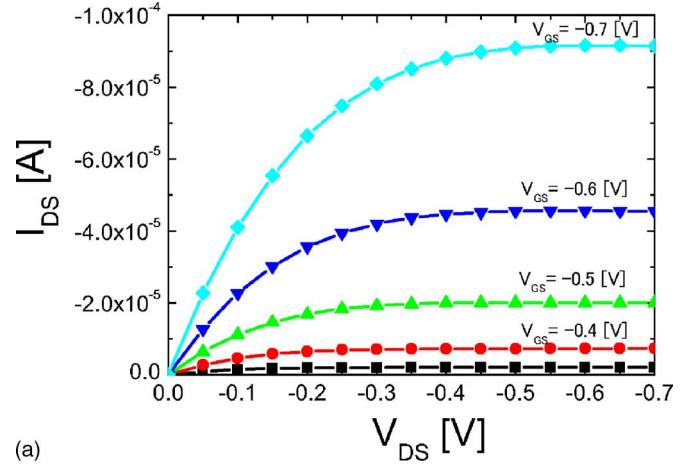
$$\Delta Q_i = \frac{\Delta Q_h C_i}{C_i + C_{dl}} \quad (2)$$

In Si-ISFETs, the capacitance of the solid side (C_i) on the channel surface can be evaluated by the thickness of the gate insulator. When the channel is covered with a 10 nm SiO₂ insulating layer, C_i is 0.345 $\mu\text{F}/\text{cm}^2$ [5]. Using the reported capacitance of a double layer (C_{dl}) of SiO₂ (20 $\mu\text{F}/\text{cm}^2$) and the above C_i , the charge increase (ΔQ_i) can be calculated by Eq. (2) and is found to be only 1.7% of the original charge change of DNA hybridization ($-\Delta Q_h$). The thick gate insulator is inevitable in the case of Si-ISFET to prevent the silicon surface from interfering ions, and this thick insulator is caused by the inefficient charge distribution. In diamond SGFETs, however, the effective thickness of the gate insulator is very thin because the channel surface is exposed directly to the solution without an insulating layer and the charge of DNA is translated directly to the channel surface. Here we estimate the capacitance of the solid side (C_i) on the diamond surface channel based on the current-voltage characteristics of metal oxide semiconductor field effect transistors (MOSFETs) because the characteristics of the SGFETs are equivalent to those of MOSFETs. The saturated drain current of MOSFETs is shown in Eq. (3a) [25],

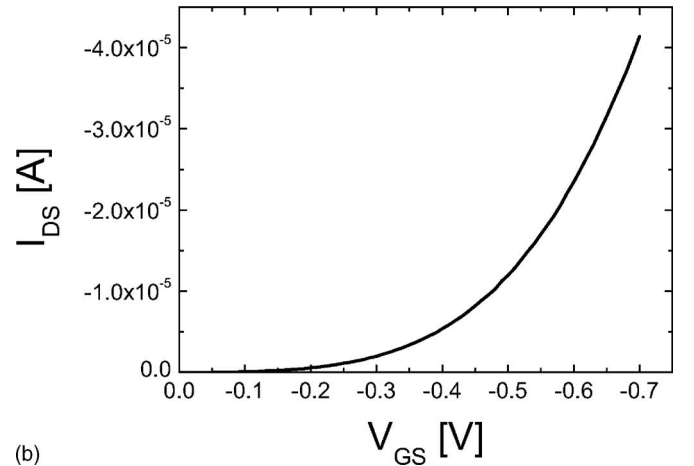
$$I_{DS} = \frac{\mu_h W C_{Tot}}{2L} (V_{GS} - V_T)^2 \quad (3a)$$

$$C_{Tot} = \frac{C_i C_{dl}}{C_i + C_{dl}} \quad (3b)$$

Since C_{Tot} is a total capacitance between the liquid side (C_{dl}) and the solid side (C_i), the C_{Tot} is a serial sum of capacitances with electric double layer ($C_{dl}=5 \mu\text{F}/\text{cm}^2$) [26] in the liquid side and the insulating layer in the solid side (C_i) on the channel surface in solution, as shown in Fig. 1(a). From the device characteristics ($I_{DS}-V_{DS}$, $I_{DS}-V_{GS}$) shown in Fig. 5, we have calculated the capacitance of the solid side (C_i) on diamond SGFETs using Eq. (3). The mobility (μ_h) of the polycrystalline diamond surface is $\sim 10 \text{ cm}^2 \text{ V}^{-1} \text{ s}^{-1}$, channel width (W) is 8 mm, and channel length (L) is 500 μm .



(a)



(b)

FIG. 5. (Color online) The device characteristics ($I_{DS}-V_{DS}$, $I_{DS}-V_{GS}$) of diamond SGFETs on the H-terminated diamond surface in PBS solution. (a) $I_{DS}-V_{DS}$ (b) $I_{DS}-V_{GS}$.

Solid-side capacitance C_i is calculated to be about 5 $\mu\text{F}/\text{cm}^2$ from Eq. (3), C_i is equivalent to be C_{dl} , and the value of $\Delta Q_i/\Delta Q_h$ is 0.5. Consequently, the charge of DNA hybridization on the channel surface in diamond SGFETs translates under the channel surface at least 50%, which is 30-fold more sensitive than that of the Si-ISFETs having a 10 nm gate SiO₂ (1.7% translation). If we miniaturize the channel length of diamond SGFETs, we can realize the DNA sensors detecting a specific DNA sequence with real time in vivo for bioscience, and we have begun the miniaturized fabrication process of diamond SGFETs.

IV. CONCLUSION

Ultrasensitive, label-free, and sequence-specific DNA sensors have been introduced through diamond SGFETs. A 21-mer complementary target oligonucleotide at a concentration of 10 pM was detected from noncomplementary oligonucleotide with excellent discrimination (16 mV), which is the lowest concentration reported in FET DNA sensors. We detected single-base mismatched DNA (100 pM) comparing the complementary DNA; the difference of shifted gate po-

tential was 3 mV. Moreover, we certified the cyclic operation of the diamond SGFET DNA sensor following denature. These diamond SGFETs are attractive from the standpoint of requiring very little concentration of DNA analysis to make active devices and have the potential to be extended larger by using MOSFET integrated arrays assembly technology. We could distinguish the complementary, noncomplementary, and 3-mer mismatched DNA at room temperature using diamond SGFETs, and we have shown concentration and annealing-time-dependent DNA hybridization sensitivity in real-time detection by characterization of the shift of the gate potential. The sensitivity of DNA hybridization depends on the concentration of target DNA and annealing time. Dia-

mond SGFET label-free DNA sensors fabricated to detect DNA point mutations associated with disease are promising for use in electronic DNA arrays and for rapid characterization of nucleic acid samples for both pharmaceutical and *in vivo* diagnostics purposes.

ACKNOWLEDGMENTS

This work was supported by a Grant-in-Aid for the Center of Excellence (COE) Research from the Ministry of Education, Culture, Sports, Science and Technology. This work was also supported in part by the Advanced Research Institute for Science and Engineering, Waseda University.

-
- [1] J. Fritz, E. B. Cooper, S. Gaudet, P. K. Sorger, and S. R. Manalis, *Proc. Natl. Acad. Sci. U.S.A.* **99**, 14142 (2002).
- [2] Z. Li, Y. Chen, X. Li, T. I. Kamins, K. Nauka, and R. S. Williams, *Nano Lett.* **4**, 245 (2004).
- [3] F. Uslu, S. Ingebrandt, D. Mayer, S. Bocker-Meffert, M. Odenthal, and A. Offenhausser, *Biosens. Bioelectron.* **19**, 1723 (2004).
- [4] D.-S. Kim, Y.-T. Jeong, H.-J. Park, J.-K. Shin, P. Choi, J.-H. Lee, and G. Lim, *Biosens. Bioelectron.* **20**, 69 (2004).
- [5] A. Poghossian, A. Cherstvy, S. Ingebrandt, A. Offenhausser, and M. J. Schoning, *Sens. Actuators B* **111-112**, 470 (2005).
- [6] D. Gerion, F. Chen, B. Kannan, A. Fu, W. J. Parak, D. J. Chen, A. Majumdar, and A. P. Alivisatos, *Anal. Chem.* **75**, 4766 (2003).
- [7] T. G. Drummond, M. G. Hill, and J. K. Barton, *Nat. Biotechnol.* **21**, 1192 (2003).
- [8] W. U. Wang, C. Chen, K. Lin, Y. Fang, and C. Lieber, *Proc. Natl. Acad. Sci. U.S.A.* **102**, 3208 (2005).
- [9] A. W. Peterson, R. J. Heaton, and R. M. Georgiadis, *Nucleic Acids Res.* **29**, 5163 (2001).
- [10] X. Su, R. Robelek, Y. Wu, G. Wang, and W. Knoll, *Anal. Chem.* **76**, 489 (2004).
- [11] J. Fritz, M. K. Baller, H. P. Lang, H. Rothuizen, P. Vettiger, E. Meyer, H.-J. Güntherodt, Ch. Gerber, and J. K. Gimzewski, *Science* **288**, 316 (2000).
- [12] K. S. Song, M. Degawa, Y. Nakamura, H. Kanazawa, H. Umezawa, and H. Kawarada, *Jpn. J. Appl. Phys., Part 2* **43**, L814 (2004).
- [13] W. Yang, O. Auciello, J. E. Butler, W. Cai, J. A. Carlisle, J. E. Gerbi, D. M. Gruen, T. Knickerbocker, T. L. Lasseter, J. N. Russell, L. M. Smith, and R. J. Hamers, *Nat. Mater.* **1**, 253 (2002).
- [14] K. Ushizawa, Y. Sato, T. Mitsumori, T. Machinami, T. Ueda, and T. Ando, *Chem. Phys. Lett.* **351**, 105 (2002).
- [15] K. S. Song, T. Sakai, H. Kanazawa, Y. Araki, H. Umezawa, M. Tachiki, and H. Kawarada, *Biosens. Bioelectron.* **19**, 137 (2003).
- [16] A. Hartl, E. Schmich, J. A. Garrido, J. Hernando, S. C. R. Catharino, S. Walter, P. Feulner, A. Kromka, D. Steinmler, and M. Stutzmann, *Nat. Mater.* **3**, 736 (2004).
- [17] Y. V. Pleskov, A. Y. Sakharova, and M. D. Krotova, *J. Electroanal. Chem. Interfacial Electrochem.* **19**, 228 (1987).
- [18] K. S. Song, Y. Nakamura, Y. Sasaki, M. Degawa, J. H. Yang, and H. Kawarada, *Anal. Chim. Acta* **573-574**, 3 (2006).
- [19] G. J. Zhang, K. S. Song, Y. Nakamura, T. Funatsu, I. Ohdomari, and H. Kawarada, *Langmuir* **22**, 3728 (2006).
- [20] B. S. Gaylord, A. J. Heeger, and G. C. Bazan, *J. Am. Chem. Soc.* **125**, 896 (2003).
- [21] Y. Belosludtsev, I. Belosludtsev, B. Iverson, S. Lemeshko, R. Wiese, M. Hogan, and T. Powdrill, *Biochem. Biophys. Res. Commun.* **282**, 1263 (2001).
- [22] J. Israelachvili, *Intermolecular & Surface Forces* (Academic Press, London, 1992).
- [23] M. L. M. Anderson, *Nucleic Acid Hybridization* (Springer, New York, 1999).
- [24] A. V. Fotin, A. L. Drobyshev, D. Y. Proudnikov, A. N. Perov, and A. D. Mirzabekov, *Nucleic Acids Res.* **26**, 1515 (1998).
- [25] S. M. Sze, *Physics of Semiconductor Devices*, 2nd ed. (Wiley, New York, 1981).
- [26] G. M. Swain, *Anal. Chem.* **65**, 345 (1993).